EXPERIMENTAL VERIFICATION OF STABILITY FOR MILLING CUTTING PROCESS OF A MAGNETICALLY SUSPENDED MILLING SPINDLE

Jin-Ho Kyung, Jong-Kweon Park
Intelligence and Precision Machine Department, Korea Institute of Machinery and Materials,
P.O.Box 101, Yusung, Daejeon 305-600, Korea
jhkyung@kimm.re.kr

ABSTRACT

The stability of milling cutting operation, which is described by linear differential-difference equations with time invariant force coefficients, is studied. The stability analysis method, that utilizes (2,2) Pade approximant as the delay function and a generalized eigenvalue problem to obtain the characteristic equation of the chatter loop, is applied to milling cutting operation of a rigid AMB milling spindle. Also, a series of milling cutting tests are conducted for various spindle rotational speeds as the axial depth of cut varies. In order to accurately predict the stability lobes by the proposed analysis method, the parameters of the cutting equation such as the damping of the AMB spindle and the cutting coefficients are evaluated experimentally. Then, the simulation results are compared to those obtained from actual milling cutting tests. The numerical predictions by the proposed analysis method were found to be in good agreement with the measurement from actual cutting.

INTRODUCTION

Presently, the machine tool spindles levitated by active magnetic bearings(AMBs) for high-speed cutting have been supplied to customers. The AMB spindles offer high productivity and high surface quality [1,2]. But, the machine tool chatter affects directly both the quality and the productivity of milling cutting works. Machine tool chatter is a self-excited vibration that is mainly caused by a regeneration of waviness on a cut surface of a workpiece [3]. Consequently, the stability analysis for machine tool chatter and the development of the efficient analysis method for the prediction of chatter are necessary in order to establish guidelines for the selection of feeds, spindle rotational speeds, and cutting depths for chatter-free cutting.

Various methods have been developed to predict the onset of chatter by many rigorous researchers. Tlusty and Polacek [4] suggested a practical stability law for orthogonal cutting systems. Merritt [5] developed a graphical analysis method for the stability boundary by plotting a gain-phase of the harmonic response functions of the cutting process and the structure on the critical loci plot. Altintas and Budak [6] presented an analytical chatter stability analysis method for end milling operations using the eigenvalue problem. But, an iteration procedure was required to search for the chatter frequencies associated with all dominant structural modes.

Anyway, cumbersome numerical manipulations are involved in most conventional analysis methods. In order to overcome such numerical difficulties, Kyung and Lee [7] suggested the chatter stability analysis method to efficiently formulate the structural dynamics of the AMB milling spindle coupled with cutting process. The proposed analysis method utilizes (2,2) Pade approximant as the delay function and a generalized eigenvalue problem (GEP) to obtain the characteristic equation of the chatter loop.

This work focuses on the experimental verification of stability for milling cutting process of the AMB spindle. A series of milling cutting tests are conducted for various spindle rotational speeds as the axial depth of cut varies, in order to search for the onset of chatter. The proposed stability analysis method as described in [7] is applied to milling operation of a rigid AMB milling spindle with one flute cemented carbide milling cutter. Then, the simulation results are compared to those obtained from actual milling cutting tests. The numerical predictions are found to be in good agreement with those obtained from actual cutting tests under various spindle rotational speeds.

CHARACTERISTIC EQUATION OF AN AMB MILLING SPINDLE

The milling spindle system under consideration is shown in Figure 1. The workpiece is an aluminum block with a rectangular cross section that is rigidly mounted on the table of a machining center along with a tool dynamometer. Orthogonal side milling operation is made on the workpiece. The milling spindle is assumed to have two degrees-of-freedom along the Y and Z axes. The AMB spindle is designed to be considerably more compliant than the workpiece supporting structure and, therefore, its dynamics dominates the chatter phenomenon.

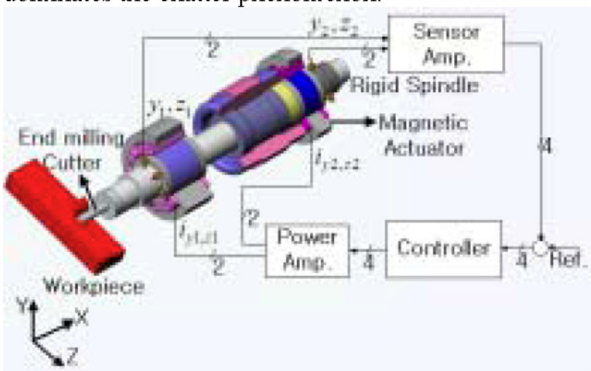

FIGURE 1: Schematic diagram of a workpiece and an AMB milling spindle

As shown in the procedure in Kyung and Lee [7], we get the characteristic equation of the chatter loop given by

$$M_c\lambda^2 + (G_c + B_c K_{amp} K_d K_s)\lambda + \frac{1}{2\mu} b K_t B_F A_0 T_c \left(e^{-\frac{T}{N}\lambda} - 1\right) + K_{cy} + B_c K_{amp} K_p K_s = 0 \quad (1)$$

where $\lambda = \sigma + i\omega$, σ and ω being the real and imaginary part of λ, respectively.

Here M_c, G_c, K_{cy}, B_F, B_c, K_p, K_d, K_{amp} and K_s denote the mass, gyroscopic, stiffness, coordinate transform, current stiffness, proportional, derivative, constant power amplifier and sensor gain matrices, respectively; K_t, b, N, μ and T are the tangential cutting coefficient, the axial depth of cut, the number of tooth, the overlap factor (μ =1 for the worst case) and the tooth period, respectively; A_o and T_c are the time invariant cutting force coefficient and coordinate transformation matrices.

Equation (1) is transcendental due to the delay element, $e^{-\frac{T}{N}\lambda}$. Then the delay function is well approximated as a rational function by the (2, 2) Pade approximant, i. e.

$$e^{-\frac{T}{N}\lambda} \cong \frac{\frac{1}{12}\left(\frac{T}{N}\right)^2 \lambda^2 - \frac{1}{2}\left(\frac{T}{N}\right)\lambda + 1}{\frac{1}{12}\left(\frac{T}{N}\right)^2 \lambda^2 + \frac{1}{2}\left(\frac{T}{N}\right)\lambda + 1} \quad (2)$$

Finally, substituting equation (2) into equation (1), the GEP can be formulated to obtain the characteristic equation described by a linear differential-difference equation.

STABILITY ANALYSIS FOR MILLING CUTTING PROCESS

The chatter stability analysis method proposed by Kyung and Lee [7] for differential-difference equations with time invariant force coefficients is employed to predict the critical depths of cut and the corresponding chatter frequencies for milling cutting operation. The stability lobe diagram can be plotted by two methods. The first method uses the relation, for seeking the lobes, given by

$$V = \frac{1}{\tilde{T}} = \frac{f}{N(n+\nu)} \quad (3)$$

Here V, n is the spindle rotational speed and an integer; ν is defined as the phase factor and has a range $0 \le \nu \le 1$; $\tilde{T}$ and f are the predicted time delay and the chatter frequency in Hz. By using the axial depth of cut, b and V from equation (3), the stability lobe diagram can be plotted. The second method predicts the unstable region (upper part of the stability lobes) using the Routh-Hurwitz criterion based on ordering the GEP into an array. Also, the chatter frequency is determined by solving the GEP.

EXPERIMENTAL PROCEDURE

The experimental apparatus is shown in Figure 2, which is composed of an AMB digital controller, a NC machining center, a Hitachi internal motor controller, an AMB milling spindle, an aluminum alloy 5052 workpiece, a Kistler tool dynamometer(9265B) and one flute end milling cutter.

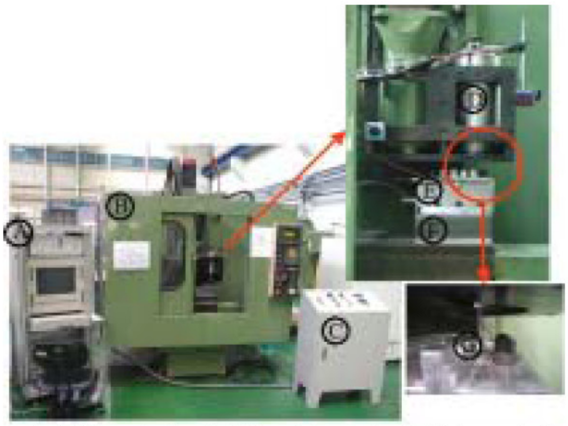

A: AMB controller, B: NC machine center, C: Motor controller, D: AMB spindle, E: Al-alloy workpiece, F: Tool dynamometer, G: One flute milling cutter

FIGURE 2: Experimental apparatus

The rotor has a length of 280 mm and an average diameter of 49.2 mm. The total mass of the rotor with one flute cemented carbide milling cutter is 4.3 kg. The position of the rotor is measured by the eddy current gap sensors which are located along the five bearing axes. The air gap of AMBs is set 0.4 *mm*. The areas of poles are 300 and 200 mm^2 for the front and rear bearings, respectively. The number of coil turns for both AMBs is 110 per leg and the bias currents in the radial bearings are 3 A.

Data acquisition and analysis were performed by a real time spectrum analyzer (AND 3565). A control algorithm was implemented on a 16-bit float point processor (TMS320C40) with a clock rate of 33 MHz. The feedback control algorithm was a conventional

PID type with low pass filter. The power amplifier delivered a maximum output current of 6 A at 48 V with a PWM frequency of 20 kHz.

SIMULATION AND EXPERIMENTAL RESULTS

Experiments for chatter vibration: During the chatter experiments, the workpiece was machined by one flute side up milling. A series of cutting tests were conducted for three different spindle rotational speeds, Ω, 5,100, 5,500 and 6,000 rpm. The feed rate was adjusted, depending on the spindle rotational speed, so as to maintain the chip thickness of 100 μm. The axial depth of cut is varied from 0.1 mm to 0.6 mm with 0.1 mm step increment. The radial depth of cut (diameter of the cutter: 6 mm) was kept 3 mm for ensuring the entry and exit immersion angles of 0 and 90 degrees, respectively. The FFT analyzer monitored the vibration of the spindle at the front bearing. During the tests, the derivative and proportional gains of the front AMBs (the rear AMBs) were kept 0.0005 and 1.6 (0.002 and 1.6).

Figure 3 shows the amplitude spectra and the time wave forms of displacements of the spindle at the front AMB for Ω = 5,100 rpm and b = 0.1 and 0.6 mm. The amplitude of the vibration response for b = 0.6 mm increases gradually with time, following the characteristic pattern of beating, which indicates the on-set of chatter vibration (see Figure 3(a)), and the power of the signal is concentrated in a narrow bandwidth around the chatter frequency, ω_c =131 Hz (see Figure 3(b)). The first peak and other small peaks in the spectrum correspond to the synchronous vibration to the spindle rotational speed and its integer-multiple harmonics. On the other hand, the time signal for b = 0.1 mm shows the stable vibration, in which any chatter related frequencies are not clearly observed. Similar results were obtained at other spindle rotational speeds, where the power of the signals were concentrated in a narrow bandwidth around the chatter frequency of ω_c = 140 Hz for Ω = 5,500 rpm and ω_c = 135 Hz for Ω = 6,000 rpm, respectively.

Figure 4 shows the minimum and maximum amplitudes of the band-pass filtered displacement signals of the spindle with respect to the chatter frequencies. The spindle rotational speed was set at 5,100 rpm and the axial depth of cut was gradually increased. The vibration amplitudes were measured and plotted against the axial depth of cut. The low vibration level observed for small depths of cut represents the background vibration level of the machine resulting from other sources of vibration such as unbalance and runouts. An abrupt increase in vibration at the axial depth of cut, b = 0.5 mm, indicates the occurrence of regenerative chatter [8].

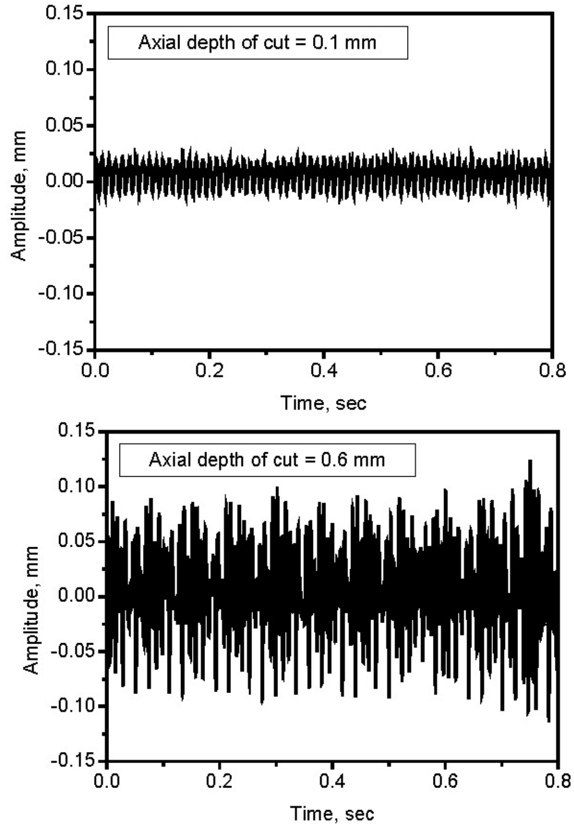

FIGURE 3(a): Time wave forms of the displacements of the spindle at Ω =5,100 rpm

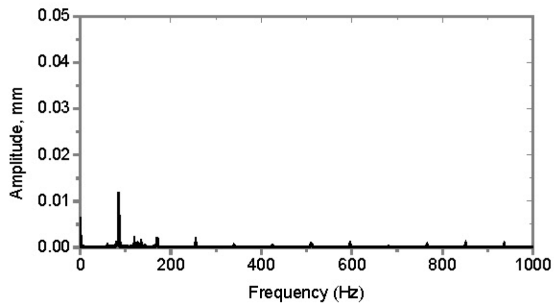

(b = 0.1 mm)

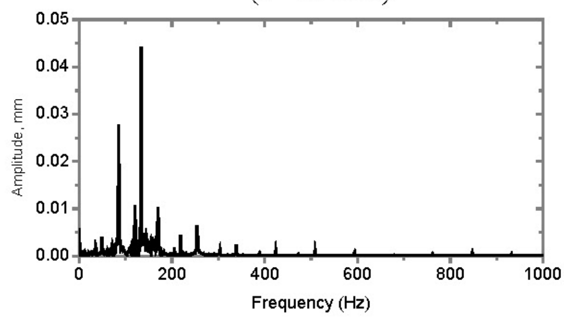

(b = 0.6 mm)

FIGURE 3(b): Amplitude spectra of the displacements of the spindle at Ω =5,100 rpm

Experimental cutting coefficients and damping: In order to accurately predict the stability lobes by the stability analysis method as shown in [7], the parameters of the cutting equation such as the cutting force coefficients, have to be evaluated experimentally.

So far, many rigorous researches have been performed to describe the machining process more accurately. Mathematical models given in Kline and Devor [9] were merged with cutting force models to predict cutting force characteristics with cutter runout for end milling. An improved model proposed in Sutherland and Devor [10] for the prediction of the cutting force system and surface error in end milling, had been developed and implemented on the computer simulation. But, these models are geometrically complicated for application because of the difficulty in seeking the parameters of the cutting equations, and the cumbersome iterative procedure to solve for the machining process. Thus, a simple direct experimental method to search the cutting coefficients is proposed in this paper as summarized below:

1) An experimental apparatus as shown in Figure 5 was prepared for the identification of the cutting force coefficients. It was comprised of a Makino NC machining center (V55), a milling spindle with ball bearings, an aluminum alloy workpiece block (Al-alloy 5052), a Kistler tool dynamometer (9257B), one flute end milling cutter and a data acquisition unit.
2) The cutting conditions were set as follows; The feed rate was varied depending on the spindle speed in order to maintain the chip thickness of 100 μm. We used the approximated instantaneous chip thickness as the true instantaneous uncut chip thickness, obtained by the procedure described in Li[11]. The axial depth of cut was changed from 0.1 mm to 0.6 mm with 0.1 mm step increment. The radial depth of cut (diameter of the cutter: 6 mm) was kept 3 mm for the entry and exit immersion angles of 0 and 90 degrees, respectively. A series of cutting tests were conducted for two different spindle rotational speeds of 5,500 rpm and 6,000 rpm.
3) The cutting forces were measured with the tool dynamometer.
4) Ensemble data sets were constructed from the measured cutting forces, and ensemble average of the data sets was calculated in order to eliminate the noise components out of the measured forces.
5) Substituting the forces in 4) into the cutting process equation shown in [7], the radial and tangential cutting forces were calculated. Steps 3) and 5) were repeated for all spindle rotational speeds and axial depths of cut of interest.
6) Substituting the radial and tangential cutting forces into the cutting process equation shown in [7], a set of cutting coefficients was calculated. An example of the calculated cutting coefficients was shown in Figure 6. Finally, the desired cutting coefficients were obtained by averaging the cutting coefficients from the set.

The measured, averaged radial and tangential force coefficients by the above procedure were 0.84 and 1.32e+9 N/m^2, respectively.

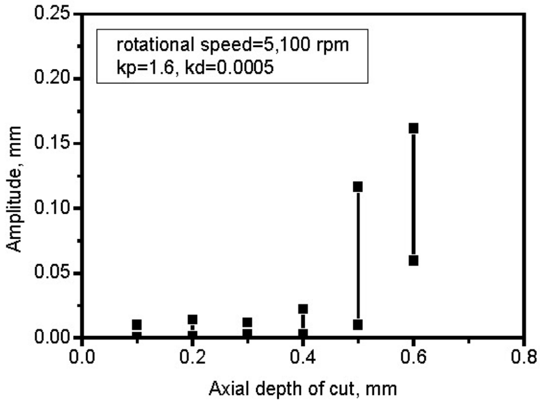

FIGURE 4: Min. and max. amplitudes of the displacements of the spindle

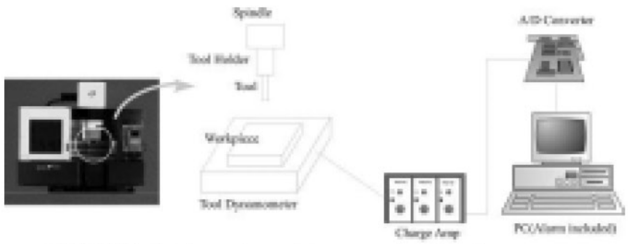

FIGURE 5: Experimental apparatus for the identification of the cutting coefficients

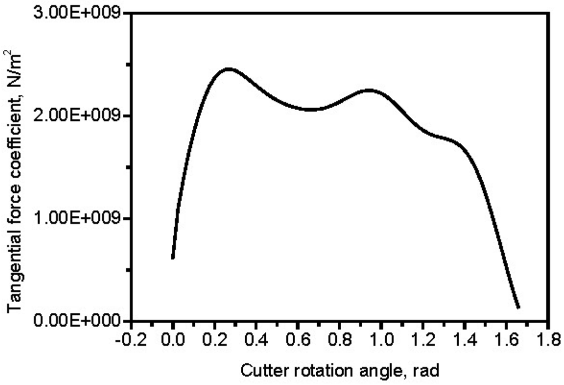

(a) Experimental tangential force coefficients

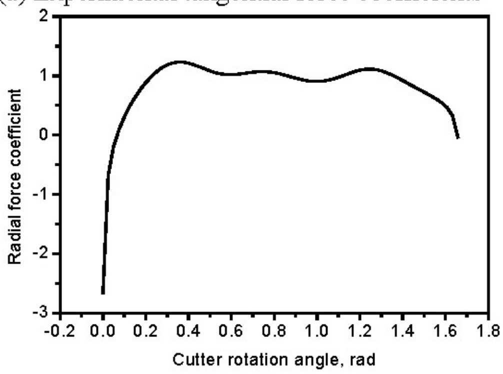

(b) Experimental radial force coefficients

FIGURE 6: Experimental force coefficients

The damping coefficient of the spindle changes depending upon milling cutting conditions. For instance, the damping coefficient during milling operation is expected to be larger than that during idle operation. The amplitude ratio of the steady-state to the static displacements is defined as the magnification factor. Figure 7 shows the frequency response functions (FRFs) of the spindle for (a) no cutting and (b) milling cutting.

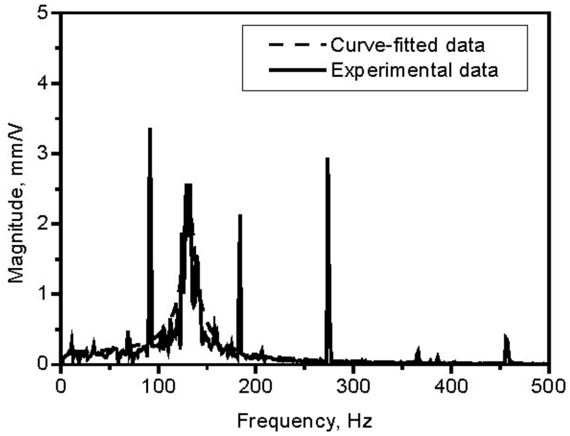

FIGURE 7(a): Measured FRF: no cutting

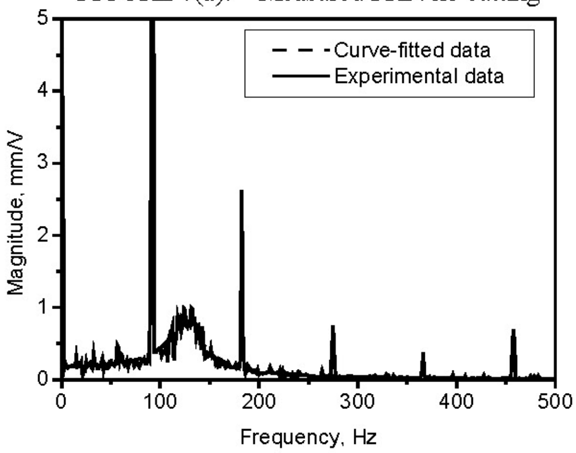

FIGURE 7(b): Measured FRF: milling cutting

An FFT analyzer estimates the FRF of the spindle at the front bearing between the displacement output and the noise input generated by a noise generator. The measured magnification factors for milling and no cuttings were 4.5 and 14, respectively. Then, the damping ratios, ζ of the spindle for milling and no cuttings were determined to be approximately 0.11 and 0.04, respectively.

The measured damping and force coefficients has to be used in the stability analysis in order to accurately predict the stability lobes.

Chatter stability analysis: Some cutting experiments were performed with the spindle rotational speed and the critical axial depth of cut varied, in order to investigate the chatter stability. At each spindle rotational speed, a series of cutting experiments were made with increasing the depth of cut, in order to search for the chatter limit and the chatter frequency. Starting from the axial depth of cut far below the probable chatter limit, the axial depth of cut was increased by the increment of 0.1 mm. The experimental critical depth of cut was determined, once chatter vibration was observed. Then the chatter frequencies were also measured.

The experimental and numerical results for three different spindle rotational speeds are shown in Figure 8. Experiments are made at the speeds and the axial depths of cut corresponding to the centers of the circles drawn in Figure 8(a). The radii of the solid circles represent the maximum amplitudes of the spindle displacement, and the radii of the dotted circles represent the maximum amplitudes of the spindle displacement that are band pass filtered with respect to the chatter frequencies. In the experiments, the axial depth of cut was gradually increased at a constant spindle rotational speed. For Ω = 5,100 rpm, a sharp increase in vibration at the axial depth of cut, b = 0.5 mm, took place, implying the occurrence of regenerative chatter. As seen in Figure 8(a), the occurrence of regenerative chatter can be detected more easily by the change of the dotted circles than by that of the solid circles. For Ω = 5,500 rpm (Ω = 6,000 rpm), the sharp increase in vibration at b = 0.5 mm (b = 0.3 mm), took place.

Since it is hard to access the exact damping ratio during cutting experiment, the measured damping ratio may not be accurate enough in actual cutting situation. Then the three dotted lines in Figure 8(a) represent the borderlines obtained from the GEP in [7] for three different damping ratios(0.11, 0.44, 0.96), which were found for three ideal cutting conditions. The measured cutting force coefficients were used in the computer simulation. Particularly, the measured value from among these damping ratios is ζ =0.11.

Figure 8(a) indicates that the predicted lobes(dotted lines) are in a fairly good agreement with the actual measurement. That is, the actual chatter limits are of order of magnitude of the limits by simulation. The discrepancy may be mainly due to the errors in damping estimation, the inaccuracy in the cutting process parameters such as the cutting force coefficients, and the unmodeled phenomena such as the formation of built-up edge, tool penetration effects and so on.

The chatter frequencies from the predictions and the measurements are compared in Figure 8(b), which shows an excellent agreement within the error less than 7 percent. In that Figure, the symbol 'o' represents the measured chatter frequencies, and the solid line means the chatter frequencies obtained by the stability analysis in case of the measured damping ratio, ζ =0.11.

SUMMARY

In this work, some milling cutting tests were carried out in the laboratory in order to validate stability for milling cutting process of the digitally controlled AMB milling spindle. The proposed stability analysis method was applied to milling operation of a rigid AMB milling spindle with one flute cemented carbide milling cutter. Then, the simulation results were compared to those obtained from actual milling cutting tests.

The accomplishments of this work can be summarized as follows:

1. A series of milling cutting tests were conducted for various spindle rotational speed as the axial depth of cut varied from 0.1 mm to 0.6 mm with 0.1 mm step increment, in order to study the chatter vibration. An abrupt increase in vibration amplitude at a certain axial depth of cut was observed, implying the occurrence of regenerative chatter.
2. In order to accurately predict the stability lobes by computer simulation, the parameters of the cutting equation such as the damping of the AMB spindle and the cutting coefficients, were determined experimentally. Particularly, a simple direct experimental method to obtain the cutting coefficients was proposed.
3. The proposed analysis method was applied to milling operation of a rigid AMB milling spindle with one flute cemented carbide milling cutter. Then, the simulation results were compared to those obtained from actual milling cutting tests. The numerical predictions of the critical depth of cut and the corresponding chatter frequency were found to be in good agreement with those from the cutting experiments under various spindle rotational speeds.

REFERENCES

1. Taniguchi, M., Ueyama, H., Nakamori, M. and Morita, N., Cutting performance of digital controlled milling AMB spindle, Fifth International Symposium on Magnetic Bearings, Kanazawa, Japan, August, pp. 375 – 379, 1996
2. IBAG Switzerland AG, A technical catalog: Motor spindles with active magnetic bearings for your HSC-applications
3. Smith, S. and Tlusty, J., Update on high-speed milling dynamics, Transactions of the ASME, Vol. 112, pp. 142 – 149, May, 1990
4. Tlusty, J. and Polacek, M., The stability of machine tools against self excited vibrations in machining, International Research in Production Engineering, ASME, pp. 465 – 474, 1963
5. Merritt, H. E., Theory of self - excited machine tool chatter, ASME Journal of Engineering for Industry, Vol. **87**, pp. 447 – 454, 1965
6. Altintas, Y. and Budak, E., Analytical prediction of stability lobes, Annals of the CIRP, Vol. **44,** pp. 357-362, 1995
7. Kyung, J. H., Lee, C. W., Controller design for a magnetically suspended milling spindle based on chatter stability analysis", JSME International Journal, Series C, Vol. 46, No. 2, pp. 416 – 422, 2003
8. Machining data handbook: third edition, Institute of Advanced Manufacturing Sciences, Inc., Ohio, USA, 1980
9. Kline, W. A. and Devor, R. E., The effect of runout on cutting geometry and forces in end milling, International Journal of Machine Tool Design and Research, Vol. 23:2/3, pp. 123-138, 1983
10. Surtherland, J. W. and Devor, R. E., An improved method for cutting force and surface error prediction in flexible end milling system, ASME Journal of engineering for industry, Vol. 108, pp. 269-279, 1986
11. Li, H. Z. and Li, X. P., A new method for determining the undeformed chip thickness in milling, Journal of Material Processing Technology, Vol. 113, pp. 378-384, 2001

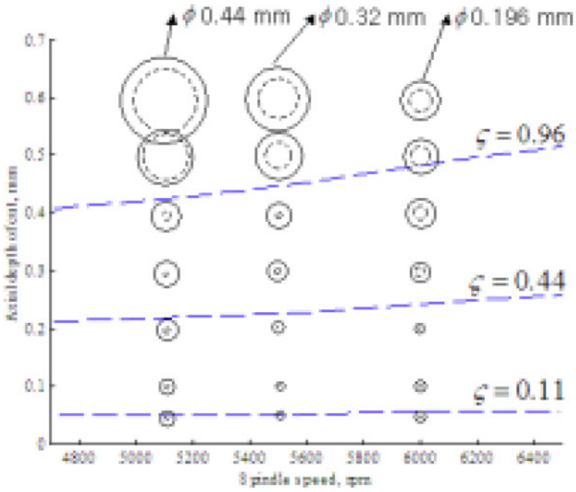

FIGURE 8(a): Simulation and experimental values of the critical depth of cut (○ : Maximum amplitudes of the displacements of the spindle, ◌ : Band-pass filtered maximum amplitudes of the displacements of the spindle at the chatter frequencies)

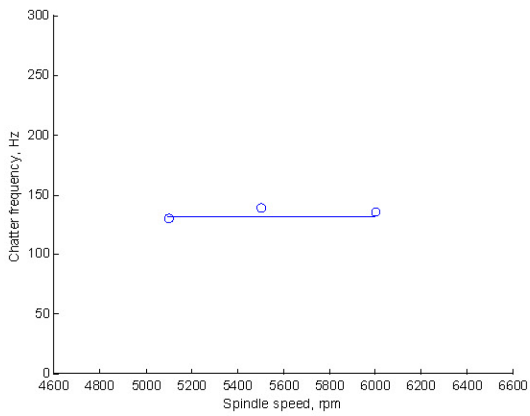

FIGURE 8(b): Simulation and experimental values of the chatter frequency